

RSC Applied Interfaces

Accepted Manuscript

This article can be cited before page numbers have been issued, to do this please use: T. Hamieh, *RSC Appl. Interfaces*, 2026, DOI: 10.1039/D6LF00006A.



This is an Accepted Manuscript, which has been through the Royal Society of Chemistry peer review process and has been accepted for publication.

Accepted Manuscripts are published online shortly after acceptance, before technical editing, formatting and proof reading. Using this free service, authors can make their results available to the community, in citable form, before we publish the edited article. We will replace this Accepted Manuscript with the edited and formatted Advance Article as soon as it is available.

You can find more information about Accepted Manuscripts in the [Information for Authors](#).

Please note that technical editing may introduce minor changes to the text and/or graphics, which may alter content. The journal's standard [Terms & Conditions](#) and the [Ethical guidelines](#) still apply. In no event shall the Royal Society of Chemistry be held responsible for any errors or omissions in this Accepted Manuscript or any consequences arising from the use of any information it contains.

Effect of Temperature Dependence of Deformation Polarizability and Ionization energy of Solvents on Surface Properties of Solid Materials

Tayssir Hamieh^{1,2,3*}

¹ Faculty of Science and Engineering, Maastricht University, 6200 MD Maastricht, The Netherlands

² Institut de Science des Matériaux de Mulhouse, Université de Haute-Alsace, CNRS, IS2M UMR 7361, F-68100 Mulhouse, France

³ Laboratory of Materials, Catalysis, Environment and Analytical Methods (MCEMA), Faculty of Sciences, Lebanese University, Beirut P.O. Box 6573/14, Lebanon

*Correspondence: t.hamieh@maastrichtuniversity.nl

Abstract

In recent studies, an original approach based on the London interaction equation has been proposed for the determination of the dispersive and polar surface properties of solid materials. The reported results revealed significant deviations in surface parameters compared with those obtained using classical methods. However, in these earlier works, the ionization energy and the deformation polarizability of solids and probe molecules were assumed to be temperature-independent.

In the present work, the effect of temperature on these two fundamental molecular parameters is investigated, and the influence of their temperature dependence on the surface properties associated with the adsorption of organic solvents on oxide materials such as alumina, titania, and magnesium oxide is examined. Inverse gas chromatography (IGC) at infinite dilution is employed to determine the net retention volumes of probe molecules, enabling the calculation of the free energy of adsorption, as well as its dispersive and polar components, the Lewis acid–base parameters, and the corresponding surface energies.

The results demonstrate that thermal variations in ionization energy and deformation polarizability—although relatively small—have a pronounced impact on surface thermodynamic parameters. In particular, changes of up to 100% are observed in the dispersive and polar components of the adsorption free energy for several probe molecules, while variations in the Lewis acid–base constants of solid surfaces reach up to 200% in the case of magnesium oxide. These findings clearly highlight the high



sensitivity of surface properties to temperature-dependent molecular parameters and emphasize the necessity of explicitly accounting for thermal effects in the analysis of surface–molecule interactions.

Keywords: Thermal effect; London equation; molecular interaction; surface energy; Lewis acid-base parameters

1. Introduction

In a previous study [1], an original method was introduced to determine the surface properties of solid materials by exploiting the London dispersion interaction energy between model organic probe molecules and solid surfaces. This approach enabled a more accurate separation of dispersive and polar contributions to the adsorption free energy, leading to a significant correction of the Lewis acid–base parameters of solid surfaces compared with classical chromatographic models. Such an improved separation is of considerable importance for the reliable prediction of physicochemical surface properties of materials and nanomaterials [1].

Inverse gas chromatography (IGC) at infinite dilution has been widely employed to quantify dispersive and polar free energies of adsorption through the measurement of retention volumes of probe molecules on solid materials [2–46]. In this framework, the standard free energy of adsorption, $\Delta G_a^0(T)$, is determined as a function of temperature. The London-equation-based approach has demonstrated clear superiority over traditional methods relying on empirical or semi-empirical solvent parameters, such as the boiling point T_{BP} [2], vapor pressure P_0 [3,4], dispersive surface tension γ_t^d [8], topological indices [6,7], standard enthalpy of vaporization ΔH_{vap}^0 , or deformation polarizability $\alpha_{0,L}$ [5].

Several subsequent studies [1,8,13–17,26,27,34] have further refined the determination of surface properties—including dispersive surface energy, polar free energy, and Lewis acid–base constants—by incorporating thermal models that account for the temperature dependence of the surface area of organic probe molecules. These developments have confirmed the essential role of temperature in surface thermodynamics.

More recently, the London-equation-based formalism introduced a new thermodynamic parameter, \mathcal{P}_{SX} , to describe solid–molecule interactions, defined as:

$$\mathcal{P}_{SX} = \frac{3}{2} \frac{N \alpha_{0S} \alpha_{0X}}{(4\pi\epsilon_0)^2} \frac{\epsilon_S \epsilon_X}{(\epsilon_S + \epsilon_X)} \quad (1)$$



63 where α_{0S} and α_{0X} are the deformation polarizabilities of the solid surface and the adsorbed mole-
64 cule, respectively, \mathcal{N} is Avogadro's number, ϵ_0 is the vacuum permittivity, and ϵ_S and ϵ_X are their
65 corresponding ionization energies. In previous applications of this model, both deformation polariza-
66 bility and ionization energy were assumed to be independent of temperature.
67 In the present work, this framework is extended by explicitly considering the temperature de-
68 pendence of deformation polarizability and ionization energy for both solids and probe mole-
69 cules. This refined approach is applied to the determination of surface properties of alumina, titania,
70 and magnesium oxide, examining its impact on the dispersive and polar components of the adsorption
71 free energy, the Lewis acid–base parameters, and the corresponding acid and base surface energies.
72 This study provides a more physically consistent description of surface–molecule interactions and
73 highlights the critical role of thermal effects in surface thermodynamic analyses.
74

75 2. Materials and Methods

76 The solid materials and organic solvents were used in previous studies [1,16,17] using chroma-
77 tographic methods and models. The non-polar organic solvents were *n*-hexane, *n*-heptane, *n*-
78 octane, and *n*-nonane, whereas the polar molecules were dichloromethane, chloroform, carbon
79 tetrachloride, benzene, ethyl acetate, diethyl ether, acetone, tetrahydrofuran (THF), acetone,
80 toluene, and acetonitrile.

81 In the context of inverse gas chromatography, molecular polarity is not solely defined by the
82 presence of a permanent dipole moment. According to the Gutmann donor–acceptor concept,
83 molecules such as benzene, toluene, and carbon tetrachloride—although nonpolar in the clas-
84 sical electrostatic sense—exhibit weak but measurable electron-donor or electron-acceptor
85 character arising from π -electron delocalization or highly polarizable bonds. These molecules
86 are therefore treated as weakly polar probes in IGC analyses, as they are capable of engaging
87 in specific Lewis acid–base interactions with solid surfaces. Table S1 summarizes the corrected
88 Gutmann donor (*DN*) and acceptor (*AN*) electron numbers together with the permanent dipole
89 moments of the probe molecules, highlighting that several solvents classified as weakly polar
90 or amphoteric in inverse gas chromatography exhibit specific Lewis acid–base character despite
91 possessing negligible or very small permanent dipole moments.

92 The solid materials were alumina (Al_2O_3), magnesium oxide (MgO), and titania (TiO_2) and
93 previously characterized [1]. Table 1 lists for all chemicals the CAS registry number, source of



94 chemicals, and reported purity. The net retention time of organic solvents adsorbed on the dif-
 95 ferent solid surfaces was determined at different temperatures using inverse gas chromatog-
 96 raphy (IGC) at infinite dilution with the help of a Focus GC gas chromatograph equipped with
 97 a flame ionization detector of high sensitivity (Sigma-Aldrich, Paris, France). A mass of 1 g of
 98 solid particles was packed into a stainless-steel column of a length of 30 cm and 2 mm internal
 99 diameter. Helium was used as carrier gas with a flow rate equal to 25 mL/min. The retention
 100 times of the different injected organic solvents were measured at infinite dilution, supposing
 101 that there is no interaction between the probe molecules themselves. The column temperatures
 102 varied from 30 to 200 °C. Average retention times and volumes were determined by repeating
 103 each solvent injection three times with a standard deviation less than 1% in all chromatographic
 104 measurements. Uncertainty propagation was evaluated by considering experimental uncertain-
 105 ties in retention times (1%), temperature control (± 0.1 K), and molecular parameters such as
 106 deformation polarizability and ionization energy. The resulting uncertainties in derived adsorp-
 107 tion energies and acid–base parameters remain within $\pm 5\%$, indicating that the observed tem-
 108 perature trends are robust and not dominated by experimental error. All reported values repre-
 109 sent the mean of repeated measurements, and the associated uncertainties are expressed as
 110 standard deviations. The number of significant figures has been adjusted to reflect the experi-
 111 mental precision.

112
 113 **Table 1.** List of probe molecules used in this study with CAS registry number, source of chem-
 114 icals, and reported purity. All chemicals were used as received without further purification.

Chemical	CAS No.	Supplier and Location	Reported Purity
n-Hexane	110-54-3	Aldrich, Paris, France	$\geq 99\%$
n-Heptane	142-82-5	Aldrich, Paris, France	$\geq 99\%$
n-Octane	111-65-9	Aldrich, Paris, France	$\geq 99\%$
n-Nonane	111-84-2	Aldrich, Paris, France	$\geq 99\%$
Dichloromethane	75-09-2	Aldrich, Paris, France	$\geq 99\%$
Chloroform	67-66-3	Aldrich, Paris, France	$\geq 99\%$
Carbon tetrachloride	56-23-5	Aldrich, Paris, France	$\geq 99\%$
Benzene	71-43-2	Aldrich, Paris, France	$\geq 99\%$
Ethyl acetate	141-78-6	Aldrich, Paris, France	$\geq 99\%$
Diethyl ether	60-29-7	Aldrich, Paris, France	$\geq 99\%$
Acetone	67-64-1	Aldrich, Paris, France	$\geq 99\%$
Tetrahydrofuran (THF)	109-99-9	Aldrich, Paris, France	$\geq 99\%$



Toluene	108-88-3	Aldrich, Paris, France	≥99%
Acetonitrile	75-05-8	Aldrich, Paris, France	≥99%
α-Alumina (Al ₂ O ₃)	1344-28-1	Aldrich, Paris, France	≥99%
Magnesium oxide (MgO)	1309-48-4	Aldrich, Paris, France	≥99%
Titanium dioxide (TiO ₂)	13463-67-7	Aldrich, Paris, France	≥99%

View Article Online
DOI: 10.1039/D6LF00006A

115

116 The IGC technique [2–46] allows the characterization of the surface properties of solid materials
117 through the determination of the net retention volumes of probe molecules adsorbed on the solid sur-
118 faces. This approach enables the determination of the free energy of adsorption ΔG_a^0 of the adsorbed
119 molecules by using the following fundamental equation of IGC:

$$120 \quad \Delta G_a^0(T) = -RT \ln V_n + C(T) \quad (2)$$

121 where V_n is the net retention volume of a probe, T the absolute temperature, R the universal
122 gas constant, and $C(T)$ a constant depending on the temperature and the parameters of interac-
123 tion between the solid and the solvent given by:

$$124 \quad C(T) = RT \ln \left(\frac{sm\pi_0}{P_0} \right) \quad (3)$$

125 where m is the mass of the solid particles, s is the specific surface area of the solid material, and P_0
126 is the reference pressure, while π_0 is the two-dimensional pressure defined in the literature accord-
127 ing to one of the following reference states:

128 - Kemball and Rideal reference state [47] given for $T_0 = 0^\circ\text{C}$ by $P_0 = 1.013 \times 10^5 \text{ Pa}$ and

$$129 \quad \pi_0 = 6.08 \times 10^{-5} \text{ N m}^{-1}.$$

130 - De Boer and Kruyer reference state [48] given for $T_0 = 0^\circ\text{C}$ by $P_0 = 1.013 \times 10^5 \text{ Pa}$ and

$$131 \quad \pi_0 = 3.38 \times 10^{-5} \text{ N m}^{-1}.$$

132 The total free energy of adsorption $\Delta G_a^0(T)$ is composed of the respective London dispersive
133 energy $\Delta G_a^d(T)$ and polar energy $\Delta G_a^p(T)$:

$$134 \quad \Delta G_a^0(T) = \Delta G_a^d(T) + \Delta G_a^p(T) \quad (4)$$

135 In a recent study, an original method based on the London dispersion interaction expression. was
136 proposed [34]. The London dispersion equation [1] was used for the determination of the free
137 dispersive energy $-\Delta G_a^d(T)$ and the fundamental equation is written as:

$$138 \quad \Delta G_a^d(T) = -\frac{3}{2} \frac{\alpha_{01} \alpha_{02}}{(4\pi\epsilon_0)^2 H^6} \frac{N \epsilon_1 \epsilon_2}{(\epsilon_1 + \epsilon_2)} \quad (5)$$

139 where α_{01} and α_{02} are the respective deformation polarizabilities of Molecules 1 and 2 sepa-
140 rated by a distance H , and ϵ_1 and ϵ_2 are the ionization energies of Molecules 1 and 2.



141 In the case of adsorption of organic solvents on solid materials, the solid molecule (Molecule
 142 1) was denoted S and the probe molecule (Molecule 2) denoted by X and combining the pre-
 143 vious equations. The free energy of adsorption $\Delta G_a^0(T)$ can be written as:

$$144 \quad \Delta G_a^0(T) = -RT \ln Vn + C(T) = -\frac{\alpha_{0S}}{H^6} \left[\frac{3N}{2(4\pi\epsilon_0)^2} \left(\frac{\epsilon_S \epsilon_X}{(\epsilon_S + \epsilon_X)} \alpha_{0X} \right) \right] + \Delta G_a^p(T) \quad (6)$$

145 A new thermodynamic parameter \mathcal{P}_{SX} was proposed as new chromatographic indicator varia-
 146 ble given by:

$$147 \quad \mathcal{P}_{SX} = \frac{3N\alpha_{0S}\alpha_{0X}}{2(4\pi\epsilon_0)^2} \frac{\epsilon_S \epsilon_X}{(\epsilon_S + \epsilon_X)}$$

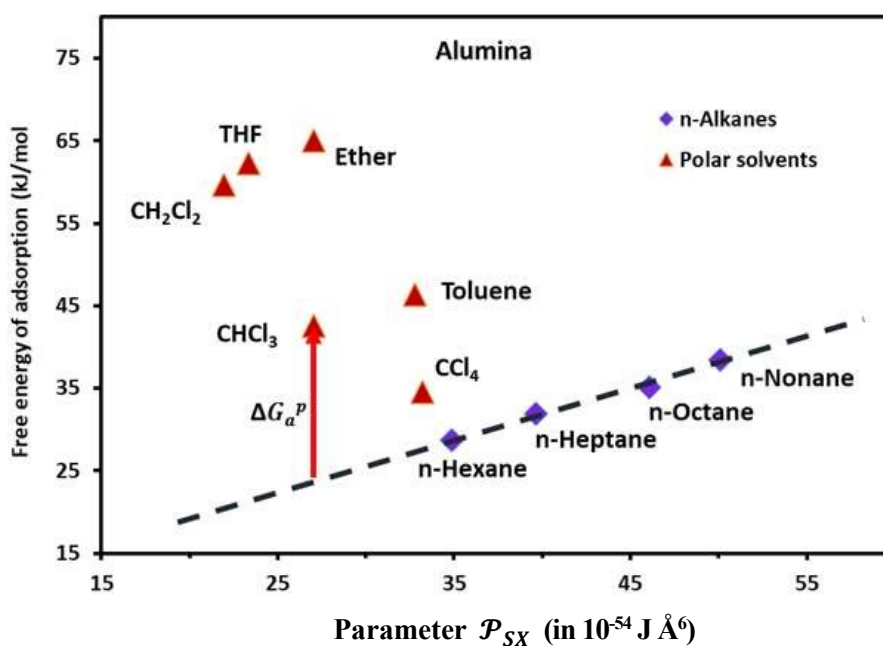
148 Equation (6) becomes as follows:

$$149 \quad \Delta G_a^0(T) = -RT \ln Vn + C(T) = -\frac{\mathcal{P}_{SX}}{H^6} + \Delta G_a^p(T) \quad (7)$$

150 The representation of $\Delta G_a^0(T)$ as a function of \mathcal{P}_{SX} led to quantify both the dispersive and polar
 151 contributions of the total free energy of adsorption using n-alkanes and polar solvents. The free energy
 152 of n-alkanes gave the dispersive component $\Delta G_a^d(T)$ because they only exhibit dispersive interac-
 153 tions, while the distance between the representative point of the polar solvent and the n-alkanes straight-
 154 line led to ΔG_a^p as it was shown in Figure 1.

155 Knowing the polar free energy of polar solvents and their total free energy, it was possible to obtain
 156 the dispersive free energy of these solvents using Equation (4). On the other hand, the application of
 157 Equation (5) to n-alkanes and polar organic molecules allowed to determine the separation distance H
 158 between the solvents and solid material.

159



160



161 **Figure 1.** Variations of the free energy ΔG_a^0 (in kJ/mol) of adsorption of organic solvents on alumina
162 surfaces as a function of the parameter \mathcal{P}_{SX} (in 10^{-54} J \AA^6) at 323.15K

163

164 In previous studies [1,26,27], the ionization energy and deformation polarizability of solid and
165 solvents were supposed constants independent from the temperature. Even if the variations of
166 these variables slightly vary versus the temperature, the temperature effect of these parameters
167 on the surface properties of solid materials was highlighted in this paper.

168 For clarity and consistency, a list of abbreviations, definitions, and units used in the theoretical
169 and thermodynamic analysis is provided in the Supporting Information.

170

171 3. Results

172 The variations of the ionization energy and deformation polarizability of the different com-
173 pounds used in this work were determined as a function of temperature using several references
174 from the literature [49-64]. Recent studies [65-70] further illustrate the growing use of elec-
175 tronic-structure descriptors (e.g., adsorption energies, reaction barriers, charge redistribution,
176 and free-energy relationships) to rationalize chemical reactivity and interfacial phenomena. For
177 example, kinetic and mechanistic analyses of gas-phase radical reactions highlight how elec-
178 tronic features and the underlying potential-energy surface govern reaction pathways and reac-
179 tivity trends [65,66]. In parallel, density functional theory (DFT) investigations have been
180 widely employed to resolve mechanistic questions by locating transition states and quantifying
181 activation energies, thereby linking molecular electronic structure to measurable thermody-
182 namic and kinetic observables [65]. DFT has also been used to analyze adsorption on carbon-
183 based substrates (e.g., defective graphene), where adsorption-induced changes in electronic
184 properties are central to sensing and interfacial response. Likewise, recent computational stud-
185 ies correlate molecular electronic properties with functional performance, including organic
186 redox/electrode behavior and acid–base descriptors derived from energetic and vibrational sig-
187 natures [70]. Collectively, these contributions emphasize that surface/interfacial properties are
188 governed by electronic quantities and their coupling to thermodynamic functions. In this con-
189 text, explicitly incorporating the temperature dependence of ionization energy and deformation



190 polarizability provides a physically consistent route to improve adsorption-energy partitioning
 191 and Lewis acid–base surface parameters obtained from inverse gas chromatography.
 192 The values of the deformation polarizability α_0 of solvents and solid materials as a function of
 193 temperature were given in Table S2 showing a slight linear increase and satisfying the following
 194 equation:

$$\alpha_0(T) = (d\alpha_0/dT)T + \alpha_0(0K) \quad (8)$$

195 where $d\alpha_0/dT$ is the temperature coefficient of polarizability and $\alpha_0(0K)$ is the deformation
 196 polarizability extrapolated at 0K. The linear equations relative to the solvents and solid surfaces were
 197 given in Table 2. It was observed that the polarizability coefficient is the highest for n-alkanes
 198 reaching $4.8 \times 10^{-43} \text{ C m}^2 \text{ V}^{-1} \text{ K}^{-1}$ for n-nonane proving the highest polarizability change with
 199 temperature.
 200

201 The uncertainties associated with the thermal coefficients $d\alpha_0/dT$ and deformation polarizability
 202 $\alpha_0(T)$ were determined by propagation of the standard deviations obtained from inverse gas chro-
 203 matography (IGC) measurements. Each probe injection was repeated three times, resulting in an over-
 204 all relative error of less than 1%.

205
 206 **Table 2.** Equations of the deformation polarizability $\alpha_0(T)$ ($\times 10^{-40} \text{ C m}^2 \text{ V}^{-1}$) of solvents and
 207 solid materials as a function of temperature with the values of the temperature coefficient of
 208 polarizability $d\alpha_0/dT$ and those of deformation polarizability $\alpha_0(0K)$ ($\times 10^{-40} \text{ C m}^2 \text{ V}^{-1}$) extrap-
 209 olated at 0K. Reported uncertainties (\pm) correspond to standard deviations obtained from the fitting
 210 procedure.

Compounds	Equation of $\alpha_0(T)$	$d\alpha_0/dT$ ($\times 10^{-3}$)	$\alpha_0(0K)$
n-Hexane	$\alpha_0(T) = 2.9 \times 10^{-3} T + 12.378$	2.9 ± 0.03	12.378 ± 0.124
n-Heptane	$\alpha_0(T) = 3.5 \times 10^{-3} T + 14.112$	3.5 ± 0.04	14.112 ± 0.141
n-Octane	$\alpha_0(T) = 4.3 \times 10^{-3} T + 16.420$	4.3 ± 0.04	16.420 ± 0.164
n-Nonane	$\alpha_0(T) = 4.8 \times 10^{-3} T + 17.876$	4.8 ± 0.05	17.876 ± 0.179
CCl ₄	$\alpha_0(T) = 2.2 \times 10^{-3} T + 11.410$	2.2 ± 0.02	11.410 ± 0.114
Nitromethane	$\alpha_0(T) = 1.3 \times 10^{-3} T + 7.822$	1.3 ± 0.01	7.822 ± 0.078
CH ₂ Cl ₂	$\alpha_0(T) = 1.2 \times 10^{-3} T + 7.660$	1.2 ± 0.01	7.660 ± 0.077
Chloroform	$\alpha_0(T) = 1.7 \times 10^{-3} T + 9.352$	1.7 ± 0.02	9.352 ± 0.094



Diethyl ether	$\alpha_0(T) = 2.1 \times 10^{-3} T + 9.900$	2.1±0.02	9.900±0.099
THF	$\alpha_0(T) = 1.8 \times 10^{-3} T + 8.602$	1.8±0.02	8.602±0.086
Ethyl acetate	$\alpha_0(T) = 2.5 \times 10^{-3} T + 9.45$	2.5±0.03	9.450±0.095
Acetone	$\alpha_0(T) = 1.1 \times 10^{-3} T + 6.762$	1.1±0.01	6.762±0.068
Acetonitrile	$\alpha_0(T) = 0.7 \times 10^{-3} T + 4.72$	0.7±0.01	4.720±0.047
Toluene	$\alpha_0(T) = 2.4 \times 10^{-3} T + 12.410$	2.4±0.02	12.410±0.124
Benzene	$\alpha_0(T) = 2.1 \times 10^{-3} T + 10.898$	2.1±0.02	10.898±0.109
Alumina	$\alpha_0(T) = 0.3 \times 10^{-3} T + 5.86$	0.3±0.00	5.860±0.059
Titania	$\alpha_0(T) = 0.7 \times 10^{-3} T + 7.71$	0.7±0.01	7.710±0.077
MgO	$\alpha_0(T) = 0.3 \times 10^{-3} T + 6.23$	0.3±0.00	6.230±0.062

211

212

213 The variations of the ionization energy $\varepsilon(T)$ of solvents and solid materials were given in Ta-
 214 ble S3 as a function of temperature. The obtained results showed very slight variations of $\varepsilon(T)$
 215 against the temperature. However, the variations of both $\alpha_0(T)$ and $\varepsilon(T)$ affect the values of the
 216 interaction parameter \mathcal{P}_{SX} versus the temperature.

217 The new method was based on the temperature effect on the chromatographic parameter \mathcal{P}_{SX}
 218 of different solvents respectively adsorbed on alumina, titania, and magnesium oxide.

219 Although the International System of Units is used as the reference framework, intermolecular
 220 distances are expressed in angstroms for convenience. Accordingly, the parameter P_{SX} is re-
 221 ported in $\text{J} \cdot \text{\AA}^6 \cdot \text{mol}^{-1}$, ensuring that the ratio P_{SX}/H^6 retains the correct unit of adsorption free
 222 energy ($\text{J} \cdot \text{mol}^{-1}$).

223 Table 3 gave the variations of $\mathcal{P}_{SX}(T)$ as a function of temperature of the adsorbed organic mole-
 224 cules on solid materials using the values given in previous paper [34]. It was observed a slight variation
 225 of $\mathcal{P}_{SX}(T)$ versus the temperature. However, there is an important variation of $\mathcal{P}_{SX}(T)$ depending on
 226 both solvents and solid surfaces. This was more elucidated in Table 4 giving the equations $\mathcal{P}_{SX}(T)$ of
 227 the different solvents with the extrapolated values of $\mathcal{P}_{SX}(0\text{K})$ at 0K. $\mathcal{P}_{SX}(0\text{K})$ largely varied from
 228 solvent to another and from solid to solid. The slope $d\mathcal{P}_{SX}(T)/dT$ which is equal to the derivative
 229 of \mathcal{P}_{SX} with respect of temperature represents a thermal expansion coefficient. The general equation
 230 was given as follows:



$$\mathcal{P}_{SX}(T) = A + BT$$

View Article Online
DOI: 10.1039/D6LF00006A

Where $A = \mathcal{P}_{SX}(0K)$ the extrapolated value of \mathcal{P}_{SX} at 0K and $B = d\mathcal{P}_{SX}(T)/dT$.

The uncertainty in $\mathcal{P}_{SX}(T)$ was determined from the propagated uncertainties of the different parameters derived from the experimental data.

Table 3. Values of parameter $\mathcal{P}_{SX}(T)$ of solvents adsorbed on of the solid materials as a function of temperature. The uncertainty associated with $\mathcal{P}_{SX}(T)$ is in the range 0.001–0.012 ($\times 10^{-54} \text{ J} \cdot \text{Å}^6 \cdot \text{mol}^{-1}$).

Parameter $\mathcal{P}_{SX}(T)$ ($\times 10^{-54} \text{ J} \cdot \text{Å}^6 \cdot \text{mol}^{-1}$) of alumina				
Temperature (K)	323.15	343.15	363.15	383.15
n-Hexane	34.885	35.073	35.261	35.450
n-Heptane	39.639	39.862	40.086	40.309
n-Octane	46.084	46.354	46.624	46.896
n-Nonane	50.093	50.393	50.693	50.993
CCl ₄	33.196	33.351	33.505	33.660
CH ₂ Cl ₂	21.941	22.029	22.118	22.206
Chloroform	27.036	27.157	27.278	27.399
Ether	27.060	27.196	27.332	27.468
THF	23.367	23.483	23.599	23.715
Ethyl acetate	26.756	26.914	27.073	27.231
Toluene	32.751	32.904	33.058	33.212
Parameter $\mathcal{P}_{SX}(T)$ ($\times 10^{-54} \text{ J} \cdot \text{Å}^6 \cdot \text{mol}^{-1}$) of titania				
Temperature (K)	323.15	343.15	363.15	383.15
n-Hexane	60.648	61.029	61.411	61.793
n-Heptane	68.759	69.207	69.656	70.107
n-Octane	79.819	80.358	80.899	81.441
n-Nonane	86.674	87.269	87.866	88.464
CH ₂ Cl ₂	38.621	38.810	39.000	39.190
Chloroform	47.612	47.867	48.122	48.379
THF	40.272	40.508	40.744	40.981



Ethyl acetate	46.454	46.770	47.087	47.405
Acetone	31.743	31.902	32.062	32.222
Benzene	50.392	50.672	50.953	51.234
Nitromethane	39.167	39.365	39.565	39.765
Acetonitrile	24.545	24.661	24.778	24.895
Parameter $\mathcal{P}_{SX}(T)$ ($\times 10^{-54}$ J $\cdot\text{\AA}^6\cdot\text{mol}^{-1}$) of MgO				
Temperature (K)	323.15	343.15	363.15	383.15
n-Hexane	41.560	41.701	41.842	41.982
n-Heptane	47.169	47.340	47.511	47.681
n-Octane	54.795	55.007	55.219	55.429
n-Nonane	59.530	59.767	60.004	60.240
CH ₂ Cl ₂	26.309	26.362	26.415	26.468
Chloroform	32.426	32.506	32.586	32.666
Diethyl ether	32.118	32.215	32.312	32.408
THF	27.712	27.794	27.877	27.958
Ethyl acetate	31.854	31.979	32.103	32.227
Acetone	21.803	21.850	21.896	21.942
Acetonitrile	16.654	16.685	16.716	16.747
Toluene	38.700	38.804	38.908	39.012

238

239

240 **Table 4.** Equations $\mathcal{P}_{SX}(T)$ of the different solvents adsorbed on solid materials with the extrapolated
 241 values of $\mathcal{P}_{SX}(0K)$ at 0K and the corresponding slopes $d\mathcal{P}_{SX}(T)/dT$. Values of \mathcal{P}_{SX} are expressed
 242 as $\times J \text{\AA}^6 \text{K}^{-1} \text{mol}^{-1}$ and T in K. The estimated standard deviations are bounded by: $\Delta\mathcal{P}_{SX}(0K) \leq$
 243 0.010 ($\times 10^{-54} \text{ J}\cdot\text{\AA}^6\cdot\text{mol}^{-1}$) and $\Delta(d\mathcal{P}_{SX}(T)/dT) \leq 0.1$ ($\times J \text{\AA}^6 \text{K}^{-1} \text{mol}^{-1}$).

Alumina			
Solvents	Equation $\mathcal{P}_{SX}(T)$	$\frac{d\mathcal{P}_{SX}(T)}{dT}$ ($\times 10^{-3}$)	$\mathcal{P}_{SX}(0K)$
n-Hexane	$\mathcal{P}_{SX}(T) = 0.0094 T + 31.843$	9.4	31.843



n-Heptane	$\mathcal{P}_{SX}(T) = 0.0112 T + 36.031$	11.2	36.031
n-Octane	$\mathcal{P}_{SX}(T) = 0.0135 T + 41.711$	13.5	41.711
n-Nonane	$\mathcal{P}_{SX}(T) = 0.015 T + 45.247$	15	45.247
CCl ₄	$\mathcal{P}_{SX}(T) = 0.0077 T + 30.696$	7.7	30.696
CH ₂ Cl ₂	$\mathcal{P}_{SX}(T) = 0.0044 T + 20.517$	4.4	20.517
Chloroform	$\mathcal{P}_{SX}(T) = 0.006 T + 25.083$	6	25.083
Ether	$\mathcal{P}_{SX}(T) = 0.0068 T + 24.866$	6.8	24.866
THF	$\mathcal{P}_{SX}(T) = 0.0058 T + 21.491$	5.8	21.491
Ethyl acetate	$\mathcal{P}_{SX}(T) = 0.0079 T + 24.196$	7.9	24.196
Toluene	$\mathcal{P}_{SX}(T) = 0.0077 T + 30.27$	7.7	30.27

Titania

Solvents	Equation $\mathcal{P}_{SX}(T)$	$d\mathcal{P}_{SX}(T)/dT$ ($\times 10^{-3}$)	$\mathcal{P}_{SX}(0K)$
n-Hexane	$\mathcal{P}_{SX}(T) = 0.0191 T + 54.481$	19.1	54.481
n-Heptane	$\mathcal{P}_{SX}(T) = 0.0225 T + 61.502$	22.5	61.502
n-Octane	$\mathcal{P}_{SX}(T) = 0.027 T + 71.085$	27	71.085
n-Nonane	$\mathcal{P}_{SX}(T) = 0.0298 T + 77.028$	29.8	77.028
CH ₂ Cl ₂	$\mathcal{P}_{SX}(T) = 0.0095 T + 35.556$	9.5	35.556
Chloroform	$\mathcal{P}_{SX}(T) = 0.0128 T + 43.483$	12.8	43.483
THF	$\mathcal{P}_{SX}(T) = 0.0118 T + 36.454$	11.8	36.454
Ethyl acetate	$\mathcal{P}_{SX}(T) = 0.0158 T + 41.333$	15.8	41.333
Acetone	$\mathcal{P}_{SX}(T) = 0.008 T + 29.164$	8	29.164
Benzene	$\mathcal{P}_{SX}(T) = 0.014 T + 45.856$	14	45.856
Nitromethane	$\mathcal{P}_{SX}(T) = 0.01 T + 35.947$	10	35.947
Acetonitrile	$\mathcal{P}_{SX}(T) = 0.0058 T + 22.658$	5.8	22.658

MgO

Solvents	Equation $\mathcal{P}_{SX}(T)$	$d\mathcal{P}_{SX}(T)/dT$ ($\times 10^{-3}$)	$\mathcal{P}_{SX}(0K)$
n-Hexane	$\mathcal{P}_{SX}(T) = 0.007 T + 39.287$	7	39.287
n-Heptane	$\mathcal{P}_{SX}(T) = 0.0085 T + 44.409$	8.5	44.409

View Article Online
DOI: 10.1039/C3AY00006A

RSC Applied Interfaces Accepted Manuscript



n-Octane	$\mathcal{P}_{SX}(T) = 0.0106 T + 51.378$	10.6	51.378
n-Nonane	$\mathcal{P}_{SX}(T) = 0.0118 T + 55.708$	11.8	55.708
CH ₂ Cl ₂	$\mathcal{P}_{SX}(T) = 0.0027 T + 25.452$	2.7	25.452
Chloroform	$\mathcal{P}_{SX}(T) = 0.004 T + 31.134$	4	31.134
Diethyl ether	$\mathcal{P}_{SX}(T) = 0.0048 T + 30.556$	4.8	30.556
THF	$\mathcal{P}_{SX}(T) = 0.0041 T + 26.386$	4.1	26.386
Ethyl acetate	$\mathcal{P}_{SX}(T) = 0.0062 T + 29.842$	6.2	29.842
Acetone	$\mathcal{P}_{SX}(T) = 0.0023 T + 21.053$	2.3	21.053
Acetonitrile	$\mathcal{P}_{SX}(T) = 0.0016 T + 16.153$	1.6	16.153
Toluene	$\mathcal{P}_{SX}(T) = 0.0052 T + 37.023$	5.2	37.023

244

245

246 The determination of polar free energy components of solvents adsorbed on solid surfaces was
 247 obtained using Equation 7 and the values of \mathcal{P}_{SX} given in Tables 3 and S4-S6. The representation
 248 of total free energy $\Delta G_a^0(T)$ (*n-alkane*) (Tables S4-S6) of n-alkanes adsorbed on solid ma-
 249 terials as a function of parameter of \mathcal{P}_{SX} n-alkanes denoted $\mathcal{P}_{S(n-alkane)}$ give the n-alkanes-
 250 straight-line (Figure 1) represented by the following equation:

$$251 \quad (-\Delta G_a^0(T))(n-alkane) = A \mathcal{P}_{S(n-alkane)} + C \quad (10)$$

252 where A is a constant depending on the separation distance H and C a parameter function
 253 of temperature.

254 When a polar solvent (X) is adsorbed, it is then characterized by its representative geometric point
 255 with two coordinates $[\mathcal{P}_{SX}; (-\Delta G_a^0(T))(X)]$. The difference between the free energy
 256 $(-\Delta G_a^0(T))(X)$ of the polar solvent and that of the fictive point located on the n-alkanes-
 257 straight-line having the same abscissa \mathcal{P}_{SX} (Figure 1), gives the corresponding polar free energy
 258 $(-\Delta G_a^p(T))(X)$ of solvent X :

$$259 \quad (-\Delta G_a^p(T))(X) = (-\Delta G_a^0(T))(X) - (A \mathcal{P}_{SX} + C) \quad (11)$$

260 Using the values of $\mathcal{P}_{SX}(T)$ given in Tables 3 and those of free energy $(-\Delta G_a^0)$ of adsorption
 261 reported in Tables S4-S6, the polar free energy $\Delta G_a^p(T)$ of the adsorbed organic solvents on
 262 solid materials were then obtained. The new values of $\Delta G_a^p(T)$ of the various solvents adsorbed
 263 on alumina, titania, and MgO were given in Table 5 as a function of temperature.



264 Table 5 showed that the lowest values of free polar interaction $\Delta G_a^p(T)$ were obtained with the tita-
 265 nium dioxide, whereas MgO gave the highest $\Delta G_a^p(T)$. However, the values of $\Delta G_a^p(T)$ relative alu-
 266 mina are not so far from the those of magnesium oxide.

267

268 **Table 5.** Variations of polar free energy $\Delta G_a^p(T)$ (kJ/mol) of adsorbed solvents on solid surfaces
 269 as a function of temperature. The relative error associated with $\Delta G_a^p(T)$ is less than 1%, as de-
 270 termined from chromatographic measurements.

Alumina				
Temperature (K)	323.15	343.15	363.15	383.15
CCl ₄	6.848	6.591	6.442	6.291
CH ₂ Cl ₂	38.946	36.464	34.334	31.831
Chloroform	18.676	16.093	13.779	11.726
Ether	41.199	39.000	37.001	35.171
THF	40.653	38.187	36.030	34.111
Ethyl acetate	43.013	40.705	38.397	36.089
Toluene	18.913	17.415	16.269	15.598
Titania				
Temperature (K)	323.15	343.15	363.15	383.15
CH ₂ Cl ₂	5.965	5.575	5.287	4.801
Chloroform	2.622	1.497	0.374	0.000
THF	4.122	2.800	1.480	0.167
Ethyl acetate	3.193	1.611	0.032	0.000
Acetone	4.943	3.228	1.515	0.000
Benzene	0.580	0.529	0.481	0.440
Nitromethane	9.723	8.353	6.985	5.619
Acetonitrile	3.610	1.506	0.000	0.000
MgO				
Temperature (K)	323.15	343.15	363.15	383.15
CH ₂ Cl ₂	39.945	38.903	37.861	36.819



Chloroform	10.589	10.026	9.635	9.248
Diethyl ether	35.873	33.635	31.689	29.375
THF	21.071	18.283	15.806	13.596
Ethyl Acetate	29.652	27.310	24.968	22.626
Acetone	46.707	44.062	41.716	39.541
Acetonitrile	46.573	43.625	41.094	38.803
Toluene	19.088	17.577	16.417	15.737

271

272

273 The determined free energy of adsorption of the polar solvents in Table 5 showed closest values
274 for MgO and alumina very larger than those of titania then proving higher polar interaction for
275 alumina and MgO.

276 The results showed in Table 5 were compared to those previously obtained without considering
277 the thermal effect on the ionization energy and deformation polarizability [1]. It was observed
278 in Table 6 an important deviation between the results of the two methods varying from 7% to
279 2665% (in the case of THF adsorbed on titania).

280

281 **Table 6.** Error percentage committed when the thermal effect of the chromatographic parame-
282 ters is neglected in adsorbed solvents on alumina, titania and MgO.

Alumina				
Temperature (K)	323.15	343.15	363.15	383.15
CCl4	95.1	97.5	98.7	-
CH ₂ Cl ₂	82.7	81.8	80.8	79.1
Chloroform	107.8	127.7	151.6	178.1
Ether	55.0	58.4	62.1	65.0
THF	1.1	2.5	3.4	4.9
Ethyl acetate	73.0	76.8	79.5	83.0
Toluene	114.3	120.4	123.6	123.6
Titania				
Temperature (K)	323.15	343.15	363.15	383.15



CH ₂ Cl ₂	57.3	65.5	76.3	84.9
Chloroform	20.0	34.9	138.5	-
THF	84.9	136.5	279.7	2665.2
Ethyl acetate	24.6	50.0	2544.8	-
Acetone	16.9	26.0	55.9	-
Benzene	859.4	693.7	489.8	232.6
Nitromethane	6.9	8.0	9.6	11.8
Acetonitrile	27.8	67.6	-	-
MgO				
Temperature (K)	323.15	343.15	363.15	383.15
CH ₂ Cl ₂	91.7	90.3	88.0	85.8
TCM	44.9	73.1	83.8	76.5
Diethyl ether	59.8	50.8	41.1	29.5
THF	9.4	36.8	70.4	111.8
Ethyl Acetate	79.0	72.1	63.5	53.5
Acetone	66.3	53.4	39.2	23.5

View Article Online
DOI: 10.1039/D6LF00006A

283

284

285 Serious consequences resulted from the above results leading to a higher disparity in the values
 286 of other surface thermodynamic parameters, particularly on the polar enthalpy and entropy of
 287 adsorption, and Lewis acid-base parameters of the solid substrates.

288 The polar enthalpy ($-\Delta H_a^p$) and entropy ($-\Delta S_a^p$) of solvents adsorbed on solid surfaces were
 289 obtained from the variations of the free energy of adsorption against the temperature using the
 290 following relation:

$$291 \quad \Delta G_a^p(T) = \Delta H_a^p - T \Delta S_a^p \quad (12)$$

292 The values of the above thermodynamic variables were given in Table 7 compared to the pre-
 293 vious results obtained without taking into account the thermal effect on the ionization energy
 294 and deformation polarizability of solvents.

295



296 **Table 7.** Comparison between the values of polar enthalpy ($-\Delta H_a^p$ in kJ mol^{-1}) and entropy
 297 ($-\Delta S_a^p$ in $\text{J K}^{-1}\text{mol}^{-1}$) of the various polar solvents adsorbed on the various solid obtained us-
 298 ing the previous method [1] and the new method, with the error percentages of the previous
 299 method.

Alumina						
Solvents	Previous results		New results		Error (%) on	Error (%) on
	$-\Delta S_a^p$ ($\text{J K}^{-1}\text{mol}^{-1}$)	$-\Delta H_a^p$ (kJ mol^{-1})	$-\Delta S_a^p$ ($\text{J K}^{-1}\text{mol}^{-1}$)	$-\Delta H_a^p$ (kJ mol^{-1})	$(-\Delta S_a^p)$	$(-\Delta H_a^p)$
CCl ₄	6.2	2.314	9.1	9.7553	31.9	76.3
CH ₂ Cl ₂	1.9	7.3421	117.4	76.843	98.4	90.4
CHCl ₃	102.8	71.989	115.8	55.971	11.2	28.6
Diethyl ether	104.6	52.207	100.4	73.55	4.2	29.0
THF	88.8	69.683	108.9	75.711	18.5	8.0
Ethyl acetate	90.4	40.683	115.4	80.305	21.7	49.3
Toluene	94.9	71.036	55.4	36.628	71.3	93.9
Titanium dioxide						
Solvents	Previous results		New results		Error (%) on	Error (%) on
	$-\Delta S_a^p$ ($\text{J K}^{-1}\text{mol}^{-1}$)	$-\Delta H_a^p$ (kJ mol^{-1})	$-\Delta S_a^p$ ($\text{J K}^{-1}\text{mol}^{-1}$)	$-\Delta H_a^p$ (kJ mol^{-1})	$(-\Delta S_a^p)$	$(-\Delta H_a^p)$
CH ₂ Cl ₂	30.7	12.146	18.9	12.084	62.4	0.5
CHCl ₃	56.4	20.818	56.2	20.780	0.4	0.2
THF	10	23.277	65.9	25.423	84.8	8.4
Ethyl Acetate	78.1	28.448	79	28.729	1.1	1.0
Acetone	85.4	32.518	85.7	32.635	0.4	0.4
Benzene	68.3	26.965	2.3	1.335	2869.6	1920.0
Nitromethane	68.5	31.846	68.4	31.829	0.1	0.1
Acetonitrile	104.6	37.37	105.1	37.586	0.5	0.6
MgO						
Solvents	Previous results		New results		Error (%) on	Error (%) on
	$-\Delta S_a^p$ ($\text{J K}^{-1}\text{mol}^{-1}$)	$-\Delta H_a^p$ (kJ mol^{-1})	$-\Delta S_a^p$ ($\text{J K}^{-1}\text{mol}^{-1}$)	$-\Delta H_a^p$ (kJ mol^{-1})	$(-\Delta S_a^p)$	$(-\Delta H_a^p)$



					382	370.4
CH ₂ Cl ₂	32.2	7.1665	52.100	56.781	382	370.4
CHCl ₃	-60.5	-24.435	22.1	17.665	373.8	238.3
Diethyl ether	105.1	19.543	107.2	70.503	2.0	72.3
Ethyl acetate	71.9	17.038	124.5	61.159	42.2	72.1
THF	95.8	7.8791	117.100	67.493	18.2	88.3
Acetone	242	62.489	119.2	85.107	103.0	26.6
Acetonitrile	81.6	2.0138	129.2	88.148	36.8	97.7
Toluene	-13.8	15.211	56.1	37.003	124.6	58.9

View Article Online
10.1039/D6LF00046A

300

301

302 The results in Table 7 led to the Lewis enthalpic acid–base constants K_A and K_D using the
303 empirical relation (13):

$$304 \quad -\Delta H^p = K_A \times DN + K_D \times AN \quad (13)$$

305 where AN and DN are, respectively, the electron donor and acceptor numbers of the polar
306 molecule [45] [46].

307 The values of K_A and K_D of solids were deduced by drawing the variations of $\left(\frac{-\Delta H^{Sp}}{AN}\right)$ versus
308 $\left(\frac{DN}{AN}\right)$ of polar solvents using Equation (14):

$$309 \quad \left(-\frac{\Delta H^p}{AN}\right) = K_A \left(\frac{DN}{AN}\right) + K_D \quad (14)$$

310

311 The same procedure was used for the determination of the Lewis entropic acidic ω_A and basic
312 ω_D constants of the various solid surfaces using Equations (15) or (16).

$$313 \quad (-\Delta S_a^p) = \omega_A DN' + \omega_D AN' \quad (15)$$

$$314 \quad \left(\frac{-\Delta S_a^p}{AN'}\right) = \omega_A \left(\frac{DN'}{AN'}\right) + \omega_D \quad (16)$$

315 The Lewis enthalpic and entropic acid-base parameters were shown in Table 8 and compared
316 to the previous results.

317

318 **Table 8.** Values of the enthalpic acid–base constants K_A and K_D and the entropic acid base
319 constants ω_A and ω_D of the various solid surfaces with the corresponding acid–base ratios,
320 using the new thermal method compared to the results of the previous method [1].

Previous results	This work
------------------	-----------



Lewis parameter	Alumina	Titania	MgO	Alumina	Titania	MgO
K_A	0.71	0.25	0.08	0.79	0.27	0.65
K_D	2.21	0.87	1.13	2.69	0.89	2.37
K_D/K_A	3.1	3.5	14	3.41	3.26	3.65
R^2	0.7301	0.9874	0.1722	0.9827	0.9895	0.9585
$10^3 \cdot \omega_A$	0.92	0.86	1.16	1.13	0.73	1.39
$10^3 \cdot \omega_D$	4.21	1.8	0.57	3.92	2.03	2.00
ω_D / ω_A	4.58	2.09	0.49	3.48	2.79	1.44
R^2	0.7739	0.9804	0.8126	0.973	0.9885	0.9754

View Article Online
DOI: 10.1039/D6LF00006A

321

322

323 The results indicate that all three solid materials exhibit an amphoteric character with a predominance
 324 of basic behavior. Alumina shows the highest enthalpic and entropic Lewis acid and base constants,
 325 followed by MgO, whereas titania presents the lowest Lewis acid and base constants. The Lewis acid–
 326 base parameters of MgO and alumina are found to be very close, while titania displays K_A and K_D
 327 values approximately three times lower than those of alumina and MgO. Comparison with previous
 328 results [1] reveals comparable K_A and K_D values for alumina and titania, but significantly different
 329 values for MgO surfaces. Moreover, the discrepancy between the two methods becomes more pro-
 330 nounced for the entropic acid–base constants ω_A and ω_D . Overall, the present approach provides a
 331 more accurate quantification of the surface properties of solid materials.

332

333 4. Discussion

334 The temperature dependence of the ionization energy and deformation polarizability of solvents ad-
 335 sorbed on alumina, titania, and MgO induces significant variations in the surface thermodynamic prop-
 336 erties, particularly in the polar component of the adsorption energy and the Lewis acid–base constants
 337 of the solid surfaces. Accordingly, a correction of the surface properties relative to the previous method
 338 was performed, clearly highlighting the strong influence of temperature on the thermodynamic param-
 339 eters governing the Lewis acid–base behavior of these materials.

340 The values of total free energy $-\Delta G_a^0(T)$ of different solvents adsorbed on solid surfaces given
 341 in Tables S4-S6 and those of the corresponding polar energy $-\Delta G_a^p(T)$ given in Table 5 led to



342 determine the London dispersive energy of adsorbed solvents as a function of temperature using
 343 the following equation:

$$344 \quad \Delta G_a^d(T) = \Delta G_a^0(T) - \Delta G_a^p(T) \quad (17)$$

345 The results are given in Table 9.

346
 347 **Table 9.** Variations of London dispersive energy $\Delta G_a^d(T)$ (kJ/mol) of adsorbed solvents on solid
 348 surfaces as a function of temperature.

Alumina				
Temperature (K)	323.15	343.15	363.15	383.15
n-Hexane	28.716	28.776	28.827	28.878
n-Heptane	31.857	31.774	31.692	31.609
n-Octane	35.117	34.813	34.510	34.207
n-Nonane	38.467	37.716	37.163	36.611
CCl ₄	27.666	27.858	27.993	28.129
CH ₂ Cl ₂	20.691	21.455	22.033	22.610
Chloroform	23.848	24.355	24.734	25.112
Ether	23.863	24.377	24.762	25.145
THF	21.575	22.277	22.808	23.338
Ethyl acetate	23.675	24.218	24.626	25.031
Toluene	47.776	47.508	46.754	45.523
Titania				
Temperature (K)	323.15	343.15	363.15	383.15
n-Hexane	12.233	11.145	10.061	8.981
n-Heptane	16.137	15.048	13.963	12.882
n-Octane	18.889	17.739	16.593	15.451
n-Nonane	21.792	20.513	19.239	17.968
CH ₂ Cl ₂	4.902	3.994	3.089	2.186
Chloroform	8.045	7.073	6.102	5.134
THF	5.479	4.571	3.665	2.761



Ethyl acetate	7.640	6.700	5.760	4.821
Acetone	2.497	1.646	0.797	
Benzene	9.017	8.026	7.037	6.050
Nitromethane	5.093	4.183	3.276	2.370
MgO				
Temperature (K)	323.15	343.15	363.15	383.15
n-Hexane	28.716	28.776	28.827	28.878
n-Heptane	31.857	31.774	31.692	31.609
n-Octane	35.117	34.813	34.510	34.207
n-Nonane	38.467	37.716	37.163	36.611
CH ₂ Cl ₂	20.718	21.478	22.056	22.631
Chloroform	23.925	24.424	24.800	25.172
Diethyl ether	23.764	24.284	24.678	25.066
THF	21.453	22.165	22.706	23.242
Ethyl Acetate	23.625	24.171	24.585	24.992
Acetone	18.355	19.315	20.047	20.775
Acetonitrile	15.656	16.839	17.744	18.645
Toluene	27.215	27.443	27.611	27.774

349

350

351 The original consequence of this new approach was the determination of the intermolecular
 352 distance $H(T)$ between the organic solvents and the solid materials as a function of tempera-
 353 ture. Indeed, using Equation (4) and the values of London dispersive free energy $-\Delta G_a^d(T)$ of
 354 adsorption of solvents on the different solid surfaces given in Table 9 against the temperature, the val-
 355 ues of the intermolecular distance $H(T)$ were obtained from the following Equations:

356

$$(-\Delta G_a^d(T)) = \frac{\mathcal{P}_{SX}(T)}{H(T)^6} \quad (18)$$

357

$$H(T) = \left[\frac{\mathcal{P}_{SX}(T)}{(-\Delta G_a^d(T))} \right]^{1/6} \quad (19)$$

358 The values of $H(T)$ were given in Table 10.

359



360 **Table 10.** Variations of the intermolecular distance $H(T)$ (in Å) of the different solvents adsorbed
 361 on solid as a function of temperature.

Alumina				
Temperature T(K)	323.15	343.15	363.15	383.15
n-Hexane	3.267	3.268	3.270	3.272
n-Heptane	3.280	3.284	3.289	3.293
n-Octane	3.309	3.317	3.325	3.333
n-Nonane	3.305	3.319	3.330	3.342
CCl ₄	3.260	3.259	3.258	3.258
CH ₂ Cl ₂	3.193	3.176	3.164	3.153
Chloroform	3.229	3.220	3.214	3.209
Ether	3.229	3.220	3.215	3.209
THF	3.205	3.190	3.180	3.171
Ethyl acetate	3.227	3.218	3.213	3.207
Toluene	2.871	2.877	2.887	2.903
Titania				
Temperature T(K)	323.15	343.15	363.15	383.15
n-Hexane	4.129	4.198	4.275	4.361
n-Heptane	4.026	4.078	4.134	4.194
n-Octane	4.021	4.068	4.118	4.172
n-Nonane	3.980	4.025	4.073	4.125
CH ₂ Cl ₂	4.461	4.619	4.825	5.116
Chloroform	4.253	4.349	4.461	4.596
THF	4.409	4.549	4.724	4.957
Ethyl acetate	4.272	4.372	4.488	4.629
Acetone	4.831	5.183	5.853	-
Benzene	4.213	4.299	4.398	4.515
Nitromethane	4.443	4.595	4.790	5.060



	MgO			
Temperature T(K)	323.15	343.15	363.15	383.15
n-Hexane	3.363	3.364	3.365	3.366
n-Heptane	3.376	3.380	3.383	3.387
n-Octane	3.406	3.413	3.420	3.427
n-Nonane	3.401	3.414	3.425	3.436
CH ₂ Cl ₂	3.291	3.246	3.068	3.066
Chloroform	3.327	3.308	3.133	3.135
Diethyl ether	3.325	3.272	2.882	2.900
THF	3.300	3.226	2.996	3.020
Ethyl acetate	3.324	3.263	2.802	2.817
Acetone	3.254	3.167	2.660	2.672
Acetonitrile	3.195	3.085	2.564	2.575
Toluene	3.353	3.327	3.098	3.105

362

363

364 The variations of $H(T)$ between the solvents and the solid substrates reported in Table 10 high-365 light a clear temperature effect on the intermolecular distance. A linear increase of $H(T)$ with366 increasing temperature is observed for n-alkanes, whereas a decrease of $H(T)$ is found for po-

367 lar solvents. The results in Table 10 also reveal significant differences in intermolecular dis-

368 tances that strongly depend on the polarity and surface characteristics of the solid materials. In

369 particular, the lowest $H(T)$ values are obtained for alumina, followed by MgO, while the high-

370 est values are observed for titania. This trend is consistent with the Lewis acid–base properties

371 of the solid surfaces, as alumina exhibits the highest acid–base constants, leading to shorter

372 intermolecular distances due to stronger van der Waals and specific interactions.

373 The temperature dependence of deformation polarizability reflects the progressive softening of

374 the electronic cloud under thermal excitation, leading to enhanced electronic deformation at the

375 solid–molecule interface. Simultaneously, the decrease in ionization energy with temperature



376 indicates a reduction of the electronic potential barrier, facilitating charge displacement and
377 polarization. Together, these effects amplify dispersive and polarization-induced interactions,
378 thereby modifying surface energy, adsorption strength, and Lewis acid–base characteristics of
379 oxide materials.

380

381

382 5. Conclusions

383 The surface properties of oxide materials such as alumina, titania, and magnesium oxide were
384 determined using a refined approach that explicitly accounts for the temperature dependence of
385 the ionization energy and deformation polarizability of probe molecules, and consequently of
386 the surface thermodynamic parameters of solid materials. Although only slight variations in
387 ionization energy and deformation polarizability of organic solvents were observed with tem-
388 perature, these changes resulted in significant differences in the calculated surface properties
389 of the oxides. In particular, marked discrepancies were found in the Lewis acid–base constants
390 obtained using the present thermal method compared with those derived from the previous ap-
391 proach, which neglected temperature effects on the dispersive and polar components of the
392 adsorption energy.

393 The substantial differences observed in the intermolecular distances between solvents and the
394 various solid substrates further confirm the superiority of the proposed method, as they reflect
395 a more physically consistent description of solid–molecule interactions.

396 Overall, these findings highlight the critical importance of incorporating temperature-depend-
397 ent electronic and polarizability effects when evaluating surface reactivity, adhesion, and inter-
398 facial interactions. From a broader materials science perspective, this work establishes a funda-
399 mental link between molecular-scale properties of probe molecules and macroscopic surface
400 behavior, providing new insights for the rational design of functional materials, surface coat-
401 ings, and nanostructured interfaces with tailored thermodynamic and interfacial properties.

402

403



404 **Funding:** This research received no external funding.

405 **Data Availability Statement:** The data presented in this study are available in the article.

406 **Conflicts of Interest:** The author declares no conflicts of interest.

407

408 References

409

- 410 1. Hamieh, T. New Progress on London Dispersive Energy, Polar Surface Interactions, and
411 Lewis's Acid–Base Properties of Solid Surfaces. *Molecules* 2024, 29, 949.
412 <https://doi.org/10.3390/molecules29050949>.
- 413 2. Sawyer, D.T.; Brookman, D.J. Thermodynamically based gas chromatographic retention
414 index for organic molecules using salt-modified aluminas and porous silica beads. *Anal.*
415 *Chem.* 1968, 40, 1847–1850. <https://doi.org/10.1021/ac60268a015>.
- 416 3. Saint-Flour, C.; Papirer, E. Gas-solid chromatography. A method of measuring surface free
417 energy characteristics of short carbon fibers. 1. Through adsorption isotherms. *Ind. Eng.*
418 *Chem. Prod. Res. Dev.* 1982, 21, 337–341. <https://doi.org/10.1021/i300006a029>.
- 419 4. Saint-Flour, C.; Papirer, E. Gas-solid chromatography: Method of measuring surface free
420 energy characteristics of short fibers. 2. Through retention volumes measured near zero
421 surface coverage. *Ind. Eng. Chem. Prod. Res. Dev.* 1982, 21, 666–669.
422 <https://doi.org/10.1021/i300008a031>.
- 423 5. Donnet, J.B.; Park, S.J.; Balard, H. Evaluation of specific interactions of solid surfaces by
424 inverse gas chromatography. *Chromatographia* 1991, 31, 434–440.
- 425 6. Brendlé, E.; Papirer, E. A new topological index for molecular probes used in inverse gas
426 chromatography for the surface nanorugosity evaluation, 2. Application for the Evaluation
427 of the Solid Surface Specific Interaction Potential. *J. Colloid Interface Sci.* 1997, 194, 217–
428 224.
- 429 7. Brendlé, E.; Papirer, E. A new topological index for molecular probes used in inverse gas
430 chromatography for the surface nanorugosity evaluation, 1. Method of Evaluation. *J. Col-*
431 *loid Interface Sci.* 1997, 194, 207–216.
- 432 8. Hamieh, T.; Schultz, J. New approach to characterise physicochemical properties of solid
433 substrates by inverse gas chromatography at infinite dilution. I. II. And III. *J. Chromatogr.*
434 *A* 2002, 969, 17–47. [https://doi.org/10.1016/S0021-9673\(02\)00368-0](https://doi.org/10.1016/S0021-9673(02)00368-0).



- 435 9. Donnet, J.B.; Custodéro, E.; Wang, T.K.; Hennebert, G. Energy site distribution of carbon
436 black surfaces by inverse gas chromatography at finite concentration conditions. *Carbon*
437 2002, 40, 163–167. [https://doi.org/10.1016/S0008-6223\(01\)00168-3](https://doi.org/10.1016/S0008-6223(01)00168-3).
- 438 10. Papirer, E.; Brendlé, E.; Ozil, F.; Balard, H. Comparison of the surface properties of graph-
439 ite, carbon black and fullerene samples, measured by inverse gas chromatography. *Carbon*
440 1999, 37, 1265–1274. [https://doi.org/10.1016/S0008-6223\(98\)00323-6](https://doi.org/10.1016/S0008-6223(98)00323-6).
- 441 11. Gamble, J.F.; Davé, R.N.; Kiang, S.; Leane, M.M.; Tobyn, M.; Wang, S.S.Y. Investigating
442 the applicability of inverse gas chromatography to binary powdered systems: An applica-
443 tion of surface heterogeneity profiles to understanding preferential probe-surface interac-
444 tions. *Int. J. Pharm.* 2013, 445, 39–46.
- 445 12. Balard, H.; Maafa, D.; Santini, A.; Donnet, J.B. Study by inverse gas chromatography of
446 the surface properties of milled graphites. *J. Chromatogr. A* 2008, 1198–1199, 173–180.
- 447 13. Hamieh, T. Study of the temperature effect on the surface area of model organic molecules,
448 the dispersive surface energy and the surface properties of solids by inverse gas chroma-
449 tography. *J. Chromatogr. A* 2020, 1627, 461372.
- 450 14. Hamieh, T.; Ahmad, A.A.; Roques-Carmes, T.; Toufaily, J. New approach to determine the
451 surface and interface thermodynamic properties of H- β -zeolite/rhodium catalysts by in-
452 verse gas chromatography at infinite dilution. *Sci. Rep.* 2020, 10, 20894.
- 453 15. Hamieh, T. New methodology to study the dispersive component of the surface energy and
454 acid–base properties of silica particles by inverse gas chromatography at infinite dilution.
455 *J. Chromatogr. Sci.* 2022, 60, 126–142. <https://doi.org/10.1093/chromsci/bmab066>.
- 456 16. Hamieh, T. Some Irregularities in the Evaluation of Surface Parameters of Solid Materials
457 by Inverse Gas Chromatography. *Langmuir* 2023, 39, 17059–17070.
458 <https://doi.org/10.1021/acs.langmuir.3c01649>.
- 459 17. Hamieh, T. Inverse Gas Chromatography to Characterize the Surface Properties of Solid
460 Materials. *Chem. Mater.* 2024, 36, 5, 2231–2244. [https://doi.org/10.1021/acs.chem-
462 mater.3c03091](https://doi.org/10.1021/acs.chem-
461 mater.3c03091).
- 462 18. Voelkel, A.; Strzemiecka, B.; Adamska, K.; Milczewska, K. Inverse gas chromatography
463 as a source of physiochemical data. *J. Chromatogr. A* 2009, 1216, 1551.
- 464 19. Al-Saigh, Z.Y.; Munk, P. Study of polymer-polymer interaction coefficients in polymer
465 blends using inverse gas chromatography, *Macromolecules* 1984, 17, 803.
- 466 20. Papadopoulou, S.K.; Panayiotou, C. Thermodynamic characterization of poly(1,1,1,3,3,3-
467 hexafluoroisopropyl methacrylate) by inverse gas chromatography. *J. Chromatogr. A* 2012,
468 1229, 230.



- 469 21. Coimbra, P.; Coelho, M.S.N.; Gamelas, J.A.F. Surface characterization of polysaccharide
470 scaffolds by inverse gas chromatography regarding application in tissue engineering, *Sur-*
471 *face and Interface Analysis*, 2019, 51 (11), 1070–1077.
- 472 22. Kołodziejek, J.; Voelkel, A.; Heberger, K. Characterization of hybrid materials by means
473 of inverse gas chromatography and chemometrics. *J. Pharm. Sci.* 2013, 102, 1524.
- 474 23. Ryan, H.M.; Douglas, J.G.; Rupert, W. Inverse Gas Chromatography for Determining the
475 Dispersive Surface Free Energy and Acid–Base Interactions of Sheet Molding Compound-
476 Part II 14 Ligno-Cellulosic Fiber Types for Possible Composite Reinforcement. *J. Appl.*
477 *Polym. Sci.* 2008, 110, 3880–3888.
- 478 24. Jacob, P.N.; Berg, J.C. Acid-base surface energy characterization of microcrystalline cel-
479 lulose and two wood pulp fiber types using inverse gas chromatography. *Langmuir* 1994,
480 10, 3086–3093.
- 481 25. Carvalho, M.G.; Santos, J.M.R.C.A.; Martins, A.A.; Figueiredo, M.M. The Effects of Beat-
482 ing, Web Forming and Sizing on the Surface Energy of *Eucalyptus globulus* Kraft Fibres
483 Evaluated by Inverse Gas Chromatography. *Cellulose* 2005, 12, 371–383.
- 484 26. Hamieh, T. The Effect of Temperature on the Surface Energetic Properties of Carbon Fibers
485 Using Inverse Gas Chromatography. *Crystals* 2024, 14, 28.
486 <https://doi.org/10.3390/cryst14010028>.
- 487 27. Hamieh, T. London Dispersive and Lewis Acid-Base Surface Energy of 2D Single-Crys-
488 talline and Polycrystalline Covalent Organic Frameworks. *Crystals* 2024, 14, 148.
489 <https://doi.org/10.3390/cryst14020148>.
- 490 28. Chtourou, H.; Riedl, B.; Kokta, B.V. Surface characterizations of modified polyethylene
491 pulp and wood pulps fibers using XPS and inverse gas chromatography. *J. Adhesion Sci.*
492 *Tech.* 1995, 9, 551–574.
- 493 29. Bogillo, V.I.; Shkilev, V.P.; Voelkel, A. Determination of surface free energy components
494 for heterogeneous solids by means of inverse gas chromatography at finite concentrations.
495 *J. Mater. Chem.* 1998, 8, 1953–1961.
- 496 30. Das, S.C.; Zhou, Q.; Morton, D.A.V.; Larson, I.; Stewart, P.J. Use of surface energy distri-
497 butions by inverse gas chromatography to understand mechanofusion processing and func-
498 tionality of lactose coated with magnesium stearate. *Eur. J. Pharm. Sci.* 2011, 43, 325–333.
- 499 31. Das, S.C.; Stewart, P.J. Characterising surface energy of pharmaceutical powders by in-
500 verse gas chromatography at finite dilution. *J. Pharm. Pharmacol.* 2012, 64, 1337–1348.



- 501 32. Bai, W.; Pakdel, E.; Li, Q.; Wang, J.; Tang, W.; Tang, B.; Wang, X. Inverse gas chromatography (IGC) for studying the cellulosic materials surface characteristics: A mini review, *Cellulose*, 2023, 30, 3379–3396, <https://doi.org/10.1007/s10570-023-05116-9>. View Article Online
DOI: 10.1039/D3LF00006A
- 502 raphy (IGC) for studying the cellulosic materials surface characteristics: A mini review,
- 503 *Cellulose*, 2023, 30, 3379–3396, <https://doi.org/10.1007/s10570-023-05116-9>.
- 504 33. Dong, S.; Brendlé, M.; Donnet, J.B. Study of solid surface polarity by inverse gas chroma-
- 505 tography at infinite dilution. *Chromatographia* 1989, 28, 469–472.
- 506 34. Hamieh, T. Temperature Dependence of the Polar and Lewis Acid–Base Properties of Poly
- 507 Methyl Methacrylate Adsorbed on Silica via Inverse Gas Chromatography. *Molecules*
- 508 2024, 29, 1688. <https://doi.org/10.3390/molecules29081688>.
- 509 35. Gamble, J.F.; Leane, M.; Olusanmi, D.; Toba, M.; Supuk, E.; Khoo, J.; Naderi, M. Surface
- 510 energy analysis as a tool to probe the surface energy characteristics of micronized materi-
- 511 als—A comparison with inverse gas chromatography. *Int. J. Pharm.* 2012, 422, 238–244.
- 512 36. Newell, H.E.; Buckton, G.; Butler, D.A.; Thielmann, F.; Williams, D.R. The use of inverse
- 513 gas chromatography to measure the surface energy of crystalline, amorphous, and recently
- 514 milled lactose. *Pharm. Res.* 2001, 18, 662–666.
- 515 37. Newell, H.E.; Buckton, G. Inverse gas chromatography: Investigating whether the tech-
- 516 nique preferentially probes high energy sites for mixtures of crystalline and amorphous
- 517 lactose. *Pharm. Res.* 2004, 21, 1440–1444.
- 518 38. Ho, R.; Hinder, S.J.; Watts, J.F.; Dilworth, S.E.; Williams, D.R.; Heng, J.Y.Y. Determina-
- 519 tion of surface heterogeneity of D-mannitol by sessile drop contact angle and finite con-
- 520 centration inverse gas chromatography. *Int. J. Pharm.* 2010, 387, 79–86.
- 521 39. Calvet, R.; Del Confetto, S.; Balard, H.; Brendlé, E.; Donnet, J.B. Study of the interaction
- 522 polybutadiene/fillers using inverse gas chromatography. *J. Chromatogr. A* 2012, 1253,
- 523 164–170.
- 524 40. Papadopoulou, S.K.; Dritsas, G.; Karapanagiotis, I.; Zuburtikudis, I.; Panayiotou, C. Sur-
- 525 face characterization of poly(2,2,3,3,3-pentafluoropropyl methacrylate) by inverse gas
- 526 chromatography and contact angle measurements *Eur. Polym. J.* 2010, 46, 202–208.
- 527 41. Dritsas, G.S.; Karatasos, K.; Panayiotou, C. Investigation of thermodynamic properties of
- 528 hyperbranched poly(ester amide) by inverse gas chromatography. *J. Polym. Sci. Polym.*
- 529 *Phys.* 2008, 46, 2166–2172.
- 530 42. Chung, D.L. *Carbon Fiber Composites*; Butterworth-Heinemann: Boston, MA, USA,
- 531 1994; pp. 3–65. ISBN: 978-0-08-050073-7, <https://doi.org/10.1016/C2009-0-26078-8>.
- 532 43. Donnet, J.B.; Bansal, R.C. *Carbon Fibers*, 2nd ed.; Marcel Dekker: New York, NY, USA,
- 533 1990; 584p. <https://doi.org/10.1201/9781482285390>.



- 534 44. Liu, Y.; Gu, Y.; Wang, S.; Li, M. Optimization for testing conditions of inverse gas chro-
535 matography and surface energies of various carbon fiber bundles. *Carbon Lett.* 2023, 33,
536 909–920. <https://doi.org/10.1007/s42823-023-00472-9>.
- 537 45. Pal, A.; Kondor, A.; Mitra, S.; Thua, K.; Harish, S.; Saha, B.B. On surface energy and acid–
538 base properties of highly porous parent and surface treated activated carbons using inverse
539 gas chromatography. *J. Ind. Eng. Chem.* 2019, 69, 432–443.
540 <https://doi.org/10.1016/j.jiec.2018.09.046>.
- 541 46. Basivi, P.K.; Hamieh, T.; Kakani, V.; Pasupuleti, V.R.; Sasikala, G.; Heo, S.M.; Pasupuleti,
542 K.S.; Kim, M.-D.; Munagapati, V.S.; Kumar, N.S.; Wen, J.-H.; Kim, C.W. Exploring ad-
543 vanced materials: Harnessing the synergy of inverse gas chromatography and artificial vi-
544 sion intelligence, *TrAC Trends in Analytical Chemistry*, 2024, 173, 117655.
545 <https://doi.org/10.1016/j.trac.2024.117655>.
- 546 47. Kemball, C.; Rideal, E.K. The adsorption of vapours on mercury I) Non –polar substances,
547 *Proceedings of the Royal Society of London. Series A*, 1946, 187, 53-73.
- 548 48. De Boer J. H., Kruyer S., Entropy and mobility of adsorbed molecules I) Procedure; atomic
549 gases on charcoal, *Proceedings of the Koninklijke Nederlandse akademie van Wetenschap-*
550 *pen*, 1952, 55, 451-463.
- 551 49. Laib, M., & Mittleman, D. M. Terahertz spectroscopy of liquid n-alkanes: Temperature
552 dependence. *Journal of Infrared, Millimeter, and Terahertz Waves*, 2010, 31(9), 1015–
553 1024.
- 554 50. Madelung, O. (Ed.). (2004). *Semiconductors: Data Handbook* (3rd ed.). Springer.
- 555 51. Barthel, J., & Buchner, R. Dielectric spectroscopy of ethers over temperature. *Journal of*
556 *Solution Chemistry*, 1995, 24(12), 1311–1327.
- 557 52. Buchner, R., Hefter, G., & Barthel, J. Dielectric relaxation of polar aprotic solvents: Tem-
558 perature and frequency dependence. *The Journal of Physical Chemistry A*, 1999, 103(1),
559 1–9.
- 560 53. Barthel, J., Buchner, R., & Münsterer, M. Static and dynamic dielectric permittivity of
561 acetonitrile. *Chemical Physics Letters*, 1995, 240(1–3), 193–200.
- 562 54. Barthel, J., & Buchner, R. Dielectric properties of aromatic hydrocarbons versus tempera-
563 ture. *Journal of Molecular Liquids*, 1995, 67(1), 1–12.



- 564 55. Barker, A. S., & Sievers, A. J. Optical studies of Al₂O₃ dielectric properties vs temperature.
565 *Reviews of Modern Physics*, 1975, 47(2), S1–S179.
- 566 56. Parker, J. H. Dielectric response of TiO₂ as a function of temperature. *Physical Review*,
567 1967, 155(3), 712–714.
- 568 57. Marcus, R. A. Electrostatic free energy and other properties of states having nonequilib-
569 rium polarization. *The Journal of Chemical Physics*, 1956, 24(5), 979–989.
570 <https://doi.org/10.1063/1.1742723>
- 571 58. Parker, J. K., & Brion, C. E. Absolute photoabsorption cross-sections and oscillator
572 strengths for valence-shell transitions in acetone and ethanol. *Chemical Physics*, 1978,
573 31(2), 317–333. [https://doi.org/10.1016/0301-0104\(78\)85118-1](https://doi.org/10.1016/0301-0104(78)85118-1)
- 574 59. Bentley, T. W., & Schleyer, P. v. R. The Grunwald–Winstein equation. *Advances in Phys-
575 ical Organic Chemistry*, 1977, 14, 1–67. [https://doi.org/10.1016/S0065-3160\(08\)60294-2](https://doi.org/10.1016/S0065-3160(08)60294-2)
- 576 60. Scaife, B.K.P., Lyons, A.W. Dielectric permittivity and pVT data of some n-alkanes. Proc.
577 R. Soc. Lond. A, 1980, 370, 193–212.
- 578 61. Scaife, B.K.P., Lyons, A.W. Density and dielectric polarizability of n-alkane liquids. *Ber.
579 Bunsenges. Phys. Chem.* 1990, 94, 758–765.
- 580 62. Kaatze, U. Complex permittivity of nitromethane as function of temperature and fre-
581 quency. *J. Chem. Phys.* 1989, 90, 3071–3077.
- 582 63. Buchner, R., Barthel, J. Dielectric relaxation of halogenated methanes as function of tem-
583 perature. *J. Mol. Liq.* 1995, 63, 21–39.
- 584 64. Barthel, J., Buchner, R. Dielectric spectroscopy of ethers over temperature. *J. Solution
585 Chem.* 1995, 24, 1311–1327.
- 586 65. Issofa, P., Njabon, E. Njankwa, S., Tchamba, T., Emadak A. Kinetic and mechanistic in-
587 sights into the atmospheric hydrogen abstraction of 3-Hydroxybutanal by chlorine. *Chem.
588 Rev. Lett.*, 2026, 11-16. doi: 10.22034/crl.2025.532470.1648
- 589 66. Behjatmanesh-Ardakani, R., Imanov, H. DFT study on the mechanism of benzimidazole
590 synthesis from phenylenediamine and formic acid: Activation energies and transition



591 states' locations. *Chem. Rev. Lett.*, 2025, 8(6), 1188-1199. doi: 10.1039/d5ra00006a

592 10.22034/crl.2025.537649.1665

593 67. Haqgu, M., Rostami, Z., Mengboev, A. DFT investigation of aflatoxin B1 adsorption on
594 vacancy-defective graphene: electronic properties and sensing potential. *Chem. Rev. Lett.*,
595 2025, 8(6), 1258-1268. doi: 10.22034/crl.2025.544347.1683

596 68. Omer, R. Anwar, A., Hussein, Y., Sultan, H. K. I., Ismail, H. K., Hamasdiq, A. F., Kareem,
597 R. Obaid Synthesis and DFT-guided evaluation of PPy-ZnFe₂O₄@Fe₃O₄ nanocomposite
598 for pharmaceutical adsorption. *J. Chem. Lett.*, 2026, 240-255. doi: 10.22034/jchem-
599 lett.2025.554966.1361

600 69. Rafiee, M. A., Javaheri, M. Theoretical Study of Benzoquinone Derivatives as Organic
601 Cathode Materials in Lithium-Ion Batteries. *J. Chem. Lett.*, 2025; 6(3), 166-174. doi:
602 10.22034/jchemlett.2025.516569.1295

603 70. Kabi, A., - K. DFT-Based Insights into Carboxylic Acid Acidity: Correlating pKa with
604 Free Energy and Vibrational Signatures. *J. Chem. Lett.*, 2025, 6(3), 212-222. doi:
605 10.22034/jchemlett.2025.543299.1340.

606

607



Data Availability Statement

The data presented in this study are available in the article.

